

Aharonov-Bohm Oscillation and Chirality Effect in Optical Activity of Single Wall Carbon Nanotubes

Fei Ye,¹ Bing-Shen Wang,² and Zhao-Bin Su^{3,1}

¹Center for Advanced Study, Tsinghua University, Beijing 100084, China

²National Laboratory of Semiconductor Superlattice and Microstructure and Institute of Semiconductor, Academia Sinica, Beijing 100083, China

³Institute of Theoretical Physics, Academia Sinica, Beijing 100080, China

We study the Aharonov-Bohm effect in the optical phenomena of single wall carbon nanotubes (SWCN) and also their chirality dependence. Specially, we consider the natural optical activity as a proper observable and derive its general expression based on a comprehensive symmetry analysis, which reveals the interplay between the enclosed magnetic flux and the tubule chirality for arbitrary chiral SWCN. A quantitative result for this optical property is given by a gauge invariant tight-binding approximation calculation to stimulate experimental measurements.

PACS numbers: 61.46.+w,73.22.-f,78.67.Ch

Aharonov-Bohm (AB) effect manifests the significance of the global nature of the vector potential in quantum theory^{1,2}. Such a geometric phase effect will result in a conductance oscillation with respect to the enclosed flux in the cylindrical conductor. This phenomenon is known as the Altshuler-Aronov-Spivak effect³. Since the discovery of carbon nanotube⁴, it provides an ideal hollow cylindrical lattice sheet with distinguished chiral structures which stimulates extensive studies^{5,6,7,8,9} in recent years. Moreover it provides a novel system for studying the interplay between the enclosed AB magnetic flux versus the chiral symmetry of the tubule. When an applied magnetic flux is threaded through, it has been shown elegantly in the tight binding approximation (TBA) (or effective mass approximation)^{10,11,12} that the fundamental gap of a single wall carbon nanotube (SWCN) is a periodic function of magnetic flux. This result is also referred to a kind of AB effect. The corresponding spectrum feature has been further analyzed in Ref.¹² where the periodicity of Van Hove singularities with respect to the magnetic flux was also addressed¹². Experimental transport studies^{13,14,15} at the finite temperature, for multi-layer carbon nanotubes, also show consistently a current oscillation with a single flux quantum ϕ_0 .

Since the SWCN may behave as either an insulator or a metallic conductor depending on its chirality as well as the strength of penetrating magnetic flux, the conventional transport study might not be appropriate for exploring the generic chirality dependence of the AB effect specially for the insulating cases. Actually, as long as the AB flux appears in the hollow SWCN, all electronic canonical momenta will acquire a corresponding vector potential. As a result, the exponential phase factor associated with each C-C link induced by the threading magnetic flux together with the orientation of the chiral trident will make for an interplay between the threading flux and chirality. Therefore the AB-type effect should appear in a variety of phenomena such as the optical properties other than the transport measurements.

In this paper, we show the AB oscillation in the natural

optical activity (or natural gyrotropy) of the SWCN with arbitrary chirality. We derive a generic expression for the natural gyrotropy based upon a systematic symmetry analysis and further complement a gauge invariant TBA calculation. It exhibits the interplay among the light polarization, tubule chirality and threaded magnetic flux and reveals the characteristic role of the chiral index¹⁷.

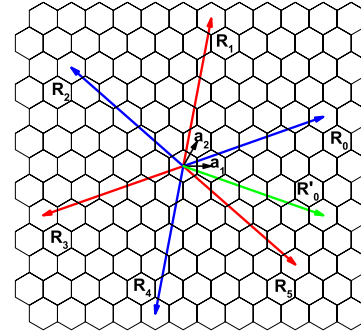


FIG. 1: For given $\mathbf{R}_0[n_1, n_2]$, there are five chiral vectors, $\mathbf{R}_1[n_1 + n_2, -n_1]$, $\mathbf{R}_2[n_2, -n_1 - n_2]$, $\mathbf{R}_3[-n_1, -n_2]$, $\mathbf{R}_4[-n_1 - n_2, n_1]$ and $\mathbf{R}_5[-n_2, n_1 + n_2]$, denoting exactly the same SWCN with their chiral angle deferred $\pi/3$ from each other successively. The tubule described by $\mathbf{R}'_0[n_1 + n_2, -n_2]$ is the mirror image of that described by \mathbf{R}_0 . \mathbf{a}_1 and \mathbf{a}_2 are 2D graphite lattice basis vectors.

An ideal SWCN can be viewed as a graphite sheet rolled up into a tubule in a fixed way along the chiral vector $\mathbf{R} = n_1\mathbf{a}_1 + n_2\mathbf{a}_2$ with \mathbf{a}_1 and \mathbf{a}_2 being the 2D graphite lattice basis vectors. Its geometric structure is hence described by a pair of integers $[n_1, n_2]$. For given $[n_1, n_2]$, there are six chiral vectors, i.e., $\mathbf{R}_0[n_1, n_2]$, $\mathbf{R}_1[n_1 + n_2, -n_1]$, ..., $\mathbf{R}_5[-n_2, n_1 + n_2]$ as shown in Fig. 1, denoting exactly the same SWCN with chiral angles (the angle between \mathbf{R} and \mathbf{a}_1) as θ , $\theta + \pi/3$, ..., $\theta + 5\pi/3$ respectively. If we introduce the chiral index $\nu \equiv \text{mod}[n_1 - n_2, 3]$ as in Ref.¹⁷, we find that they can be divided into two subsets, one is $\{\mathbf{R}_0, \mathbf{R}_2, \mathbf{R}_4\}$ with the same ν and the other is $\{\mathbf{R}_1, \mathbf{R}_3, \mathbf{R}_5\}$ with an opposite ν . The essence of this obvious but nontrivial property,

the same SWCN with opposite chiral indices, lies in the sameness of the two in-cell carbon atoms A and B. Actually this is the heritage to the carbon tubule inherited from the $6mm$ symmetry of the graphite sheet which has the $3m$ symmetry as its invariant subgroup with corresponding quotient groups as E and C_2 (or σ). C_2 (or σ) will reverse the A and B atoms and also the sign of chiral index. As a direct result of the above analysis, the physical quantities of SWCN can be written as a periodical function of θ with period $2\pi/3$ for $\nu = \pm 1$ and $\pi/3$ for $\nu = 0$, which are the consequences of the $3m$ symmetry and $6mm$ symmetry, respectively. When performing Fourier expansion for these physical quantities with respect to θ , all the expansion coefficients should be functions of those invariant quantities such as the length of chiral vector $\Lambda|\mathbf{a}_1|$ ($\Lambda = \sqrt{n_1^2 + n_2^2 + n_1n_2}$) and the greatest common divisor of n_1 and n_2 (denoted by N).

Since the rotation of the linear polarized light travelling through SWCN along the tubule axis carries the information of its chiral structure and the enclosed magnetic flux, we consider the optical rotation power (ORP), i.e., the rotation angle per unit length, as an observable to investigate the interplay between chirality and threaded magnetic flux for the SWCN. By fixing the direction of the incident light with frequency ω parallel to the tubule axis (z -axis), the ORP has the expression as¹⁶

$$\chi \equiv \omega^2 g_{xyz} / (2c^2) \quad (1)$$

where c is the light speed and the third rank tensor g_{xyz} is the derivative of the xy component of dielectric tensor with respect to q_z in the long wavelength limit $\mathbf{q} \rightarrow 0$, i.e., $g_{xyz} = \partial \varepsilon_{xy} / (i \partial q_z) |_{q \rightarrow 0}$ ¹⁶. Notice that a SWCN and its mirror image with respect to the horizontal plane possess the same chiral index, but different chiral angle θ and $-\theta$, respectively (see Fig. 1). Further taking consideration of the third rank tensor properties, one can see that χ^ν should be an odd function of θ . Hence, it has a Fourier series with only odd parity sine functions

$$\begin{aligned} \chi^\pm(\theta) &= a_1^\pm \sin(3\theta) + a_2^\pm \sin(6\theta) + a_3^\pm \sin(9\theta) + \dots, \\ \chi^0(\theta) &= a_2^0 \sin(6\theta) + a_4^0 \sin(12\theta) + \dots, \end{aligned} \quad (2)$$

where the superscripts \pm or 0 denote the chiral index, and the coefficients a_n^ν depend on the curvature, the magnetic flux and the frequency of incident light. As a natural consequence of Eq. (2) the ORP of zigzag ($\theta = 0$) and armchair ($\theta = \pi/6$) tubules is zero. Moreover, considering the rotation of \mathbf{R} by $\pi/3$, since \mathbf{R}_0 and \mathbf{R}_1 correspond to the same SWCN with opposite ν , it is straightforward to see $\chi^\pm(\theta + \pi/3) = \chi^\mp(\theta)$. Hence, we have

$$a_n^\pm(\omega, \Lambda; \phi) = (-1)^n a_n^\mp(\omega, \Lambda; \phi). \quad (3)$$

We further adopt the scheme developed by White *et al.*¹⁸, which exhibits the chiral structure of SWCN explicitly with cylindrical geometry being properly built in. In this scheme, all the lattice sites can be generated by repeating the pure rotation C_N and the screw operation

$S(\alpha, h)$, while the latter one is shifting along the tubule axis by h with a simultaneous rotation around the tubule axis by α . h and α can be obtained through equation $h = \sqrt{3}N|\mathbf{a}_1|/2\Lambda$, $\alpha = (2p_1n_1 + 2p_2n_2 + p_1n_2 + p_2n_1)\pi/\Lambda^2$ with integers p_1, p_2 satisfying $p_2n_1 - p_1n_2 = N$. Hence, the Bloch momenta $\kappa \in [-\pi, \pi)$ and $n = 0, 1, \dots, N-1$ as good quantum numbers can be extracted from the characters of the $U(1)$ -representations of $S(\alpha, h)$ and C_N , respectively. If the magnetic flux is threaded through the SWCN, the space displacement groups $S(\alpha, h)$ and C_N will be replaced by the corresponding magnetic displacement groups, which are again commutable to the Hamiltonian of the flux threaded SWCN. The Bloch momenta then become $n + \phi/\phi_0$ and $\kappa + \alpha(\phi/\phi_0)$, respectively. This provides the generic way of the flux dependence for all the gauge invariant energy spectra¹⁹ as well as matrix elements of physical quantity. As a result, the flux dependence of the observable for intrinsic SWCNs will exhibit an AB oscillation with a flux period ϕ_0 . This can be easily seen from the fact that, these quantities can be often expressed as a double summations over κ and n , the former sums over $[-\pi, \pi)$ and then smears the flux dependence via $\kappa + \alpha(\phi/\phi_0)$ while the latter summation will contribute the AB type flux dependence. Then we conclude that a_n^ν in Eq. (2) are periodic functions of ϕ

$$a_n^\nu(\omega, \Lambda; \phi) = a_n^\nu(\omega, \Lambda; \phi + \phi_0). \quad (4)$$

Equations (2), (3) and (4) complete the generic symmetry analysis for the ORP.

Now we apply the TBA to the SWCN with arbitrary given pair of $[n_1, n_2]$, and ignore the curvature effect for convenience. The TBA Hamiltonian for the SWCN with threading flux along the tubule axis can be written as a 2×2 matrix form in the momentum space

$$\mathcal{H}(\kappa, n) = V_0 \begin{bmatrix} 0 & \gamma_n^*(\kappa) \\ \gamma_n(\kappa) & 0 \end{bmatrix} \quad (5)$$

with V_0 being the transfer integral equal to 2.6 eV. The off-diagonal matrix element has the form $\gamma_n(\kappa) = 1 + e^{-i\beta_1} + e^{i\beta_2}$ with $\beta_1 = \frac{n_1}{N}(\kappa + \alpha\frac{\phi}{\phi_0}) - \frac{2\pi p_1}{N}(n + \frac{\phi}{\phi_0})$ and $\beta_2 = \frac{n_2}{N}(\kappa + \alpha\frac{\phi}{\phi_0}) - \frac{2\pi p_2}{N}(n + \frac{\phi}{\phi_0})$. Then it is straightforward to obtain the energy spectrum $E_n^{(c,v)}(\kappa) = \pm V_0 |\gamma_n(\kappa)|$ ¹¹ and the one-particle wave function for the conducting or valence band reads

$$|\kappa, n, c(v)\rangle = \frac{1}{\sqrt{2}} \left(|\kappa, n, A\rangle \pm \frac{\gamma_n(\kappa)}{|\gamma_n(\kappa)|} |\kappa, n, B\rangle \right), \quad (6)$$

where the plus and minus signs correspond to the conducting band and the valence band, respectively. The Bloch sum in Eq. (6) reads

$$|\kappa, n, s\rangle = \frac{1}{\sqrt{2MN}} \sum_{l=1}^N \sum_{m=-M}^M e^{i\kappa m + i2nl\pi/N} |m, l, s\rangle, \quad (7)$$

with s being the index of two in-cell atoms and $2Mh$ the tubule length. In Eq. (7) local state $|m, l, s\rangle$ of unit cell

(m, l) can be obtained from the $(0, 0)$ unit cell $|0, 0, s\rangle$ by m successive screw operations $S(\alpha, h)$ combined with l successive rotations C_N as $|m, l\rangle = T_{m,l}|0, 0\rangle$ with $T_{m,l} \equiv S^m(\alpha, h)C_N^l$.

For purpose of ORP calculation, we start from the off-diagonal element of the dielectric tensor $\varepsilon_{xy}(q, \omega)$,

$$\varepsilon_{xy} = \frac{8\pi e^2}{m^* \omega^2 V} \sum_{\kappa n \sigma} \sum_{\kappa' n' \sigma'} (f(E_{n'}^{\sigma'}(\kappa')) - f(E_n^\sigma(\kappa))) \times \frac{\langle \kappa n \sigma | Q_x(-q) | \kappa' n' \sigma' \rangle \langle \kappa' n' \sigma' | Q_y(q) | \kappa n \sigma \rangle}{\hbar \omega + E_n^\sigma(\kappa) - E_{n'}^{\sigma'}(\kappa') + i\epsilon}, \quad (8)$$

with σ the band index c or v . Here, m^* and e are the electron mass and charge respectively. $V \equiv \rho \cdot Mh|\mathbf{R}|^2/(2\pi)$ is the system volume with ρ as the filling factor. At zero temperature $f(E)$ is simply the step function and the vector operator $\mathbf{Q}(q)$ has the form $[\mathbf{p} + e\mathbf{A}/c, e^{iqz}]_+/2$ whose x and y components transform under symmetry operation $T_{m,l}$ as

$$\begin{aligned} & T_{m,l}^\dagger [Q_x(q) \pm iQ_y(q)] T_{m,l} \\ &= e^{imqh \pm i(m\alpha + l\pi/N)} [Q_x(q) \pm iQ_y(q)]. \end{aligned}$$

One then obtain the matrix elements of $Q_x \pm iQ_y$ between the conducting and valence bands to be

$$\begin{aligned} & \langle \kappa', n', c | Q_x(q) \pm iQ_y(q) | \kappa, n, v \rangle = \delta_{\kappa', \kappa + qh \pm \alpha} \delta_{n', n \pm 1} \\ & \times \sum_{m,l} \exp \left[-i(\kappa \pm \alpha + qh)m - i\frac{2(n \pm 1)\pi}{N}l \right] \\ & \times \langle m, l, c | Q_x(q) \pm iQ_y(q) | 0, 0, v \rangle, \quad (9) \end{aligned}$$

here the summation is over the nearest neighbors of the $(0, 0)$ unit cell and it reflects the local geometric structure of SWCN. The δ -function in Eq. (9) gives the selection rule for the transverse optical transition. To keep the gauge invariance, we transfer the calculation of the momentum matrix element into that of the co-ordinate matrix element through the commutation law $\mathbf{p} + e\mathbf{A}/c = m^*[\mathbf{r}, H]/(i\hbar)^{20}$ to avoid the explicit treatment of vector potential \mathbf{A} . The translational invariance is also rigorously kept in our calculating procedure. Based upon all the above considerations, the ORP can be calculated as

$$\begin{aligned} \chi &= \frac{e^2 \omega^2 V_0^2}{\pi \rho c^2} \sum_{n=1}^N \int_{-\pi}^{\pi} d\kappa \frac{W(\kappa, n) \Delta(\kappa, n) \partial_\kappa D(\kappa, n)}{[(\hbar \omega + i\epsilon)^2 - \Delta(\kappa, n)^2]^2}, \\ W(\kappa, n) &= 1 - \text{Re} \left[\frac{\gamma_n(\kappa) \gamma_{n+1}^*(\kappa + \alpha)}{|\gamma_n(\kappa)| |\gamma_{n+1}(\kappa + \alpha)|} e^{-i\varphi_{AB}} \right], \\ D(\kappa, n) &= |\gamma_{n+1}(\kappa + \alpha)|^2 - |\gamma_n(\kappa)|^2, \\ \Delta(\kappa, n) &= E_{n+1}^{(c)}(\kappa + \alpha) - E_n^{(v)}(\kappa), \quad (10) \end{aligned}$$

where $\varphi_{AB} = \pi(n_1 + n_2)\Lambda^{-2}$ is the difference between the azimuth angles of the two atoms in one unit cell.

In the optical limit $q \rightarrow 0$ the minimum of $\Delta(\kappa, n)$ gives an indirect band gap for the transverse optical transition

as $\Delta_g = \sqrt{3}\pi V_0/\Lambda$. This gap sets a lower bound of the incident light wavelength as $\lambda_c = 2\hbar c\Lambda/(\sqrt{3}V_0)$, below which no optical transverse absorption take place. *Since this threshold is independent of chirality, it provides a means to determine the tubule diameter for all kinds of SWCNs by optical measurements.*

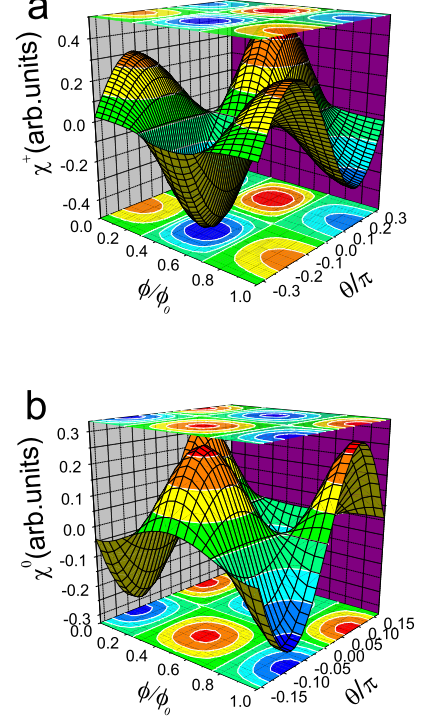


FIG. 2: The dependence of the ORP on magnetic flux and chiral angle is plotted in (a) for $\nu = 1$ and in (b) for $\nu = 0$. The normalized incident light frequency is $\bar{\omega} = 0.5$ and the tubule diameter is around 37 nm. In (a) the ORP for $\nu = 1$ tubules is a periodic function of chiral angle with period $2\pi/3$ and magnetic flux with period ϕ_0 . The ORP for $\nu = -1$ tubules can be obtained through the translation of chiral angle by $\pi/3$ in (a). In (b), the ORP for the $\nu = 0$ tubules is a periodic function of chiral angle with period $\pi/3$ and magnetic flux with period ϕ_0 .

When plotting χ versus the chiral angle θ for arbitrary $[n_1, n_2]$, we found the numerical data can be interestingly regrouped into three categories in accordance with the chiral index $\nu = 0, \pm 1$. By introducing a rescaled dimensionless frequency $\bar{\omega} = \hbar\omega/\Delta_g$, χ^ν can be fitted perfectly by the following functions with parameter $f = 4\omega^2 e^2/\pi\rho c^2 V_0$

$$\begin{aligned} \chi^\pm/f &\approx a_1^\pm(\bar{\omega}, \frac{\phi}{\phi_0}) \sin(3\theta) + \Lambda^{-1} a_2^\pm(\bar{\omega}, \frac{\phi}{\phi_0}) \sin(6\theta), \\ \chi^0/f &\approx \Lambda^{-1} a_2^0(\bar{\omega}, \frac{\phi}{\phi_0}) \sin(6\theta), \quad (11) \end{aligned}$$

where $a_1^\pm = -a_1^\mp$ and $a_2^\pm = a_2^\mp$ which, as dimensionless functions of $\bar{\omega}$ and ϕ/ϕ_0 , can be determined numerically.

Eq. (11) is entirely consistent with the above symmetry analysis (Eqs. (2) and (3)). In Fig. 2 we give 3D plots of χ^+ and χ^0 versus magnetic flux and chiral angle. Note that χ^- can be obtained through exact relation $\chi^-(\theta) = \chi^+(\theta + \pi/3)$. The results explicitly shows AB oscillation in the ORP with a single flux quantum period and χ^ν is an even function of ϕ . For large Λ , the numerical data verifies $\chi^+ = -\chi^-$ within its precision and χ^0 is much smaller than χ^\pm in magnitude (see also Eq. (11)). It is interesting to note that for $\nu = \pm 1$ tubules the magnitude of χ^\pm reaches its maximum/minimum when chiral angle approach $\pi/6$ for fixed ϕ and $\bar{\omega}$, however for the armchair tubules ($\theta = \pi/6$) $\chi^0 = 0$. This implies that the chiral index plays a role much more sensitive than the chiral angle in the natural gyrotropy properties of SWCN.

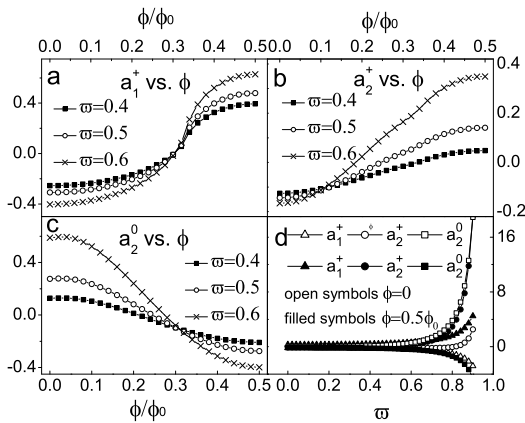


FIG. 3: Coefficients a_1^+ , a_2^+ , and a_2^0 are plotted as functions of magnetic flux ϕ for different values of renormalized frequency $\bar{\omega}$ in (a), (b), and (c), respectively. The filled square, open circle and cross symbol correspond to $\bar{\omega} = 0.4, 0.5$ and 0.6 , respectively. Fig.(d) is the plot of a_1^+ , a_2^+ , and a_2^0 vs. $\bar{\omega}$ denoted by triangle, circle and square, respectively, for different values of magnetic flux. The open symbols are the data for $\phi = 0$ and the filled symbols for $\phi = 0.5\phi_0$.

The fitting coefficients a_1^+ , a_2^+ , and a_2^0 are plotted in

Figs. 3a, 3b, and 3c respectively as the functions of ϕ/ϕ_0 with $\bar{\omega} = 0.4, 0.5, 0.6$. All a_1^+ with different $\bar{\omega}$ coincide approximately at a common node $\phi/\phi_0 = 0.31$, i.e., coincide at $\pm 0.31 + \mu$ with μ being the integer, since it is a periodic even function of ϕ/ϕ_0 . However, for the $\nu = 0$ tubules, the position of the zero point changes distinctively versus $\bar{\omega}$. Since a_1^+ dominates the χ function, this remarkable fact provides a way to distinguish experimentally whether the SWCN under investigation belong to $\nu = \pm 1$ or $\nu = 0$. In Fig. 3d we plotted a_1^+ , a_2^+ , a_2^0 as functions of $\bar{\omega}$ for fixed $\phi/\phi_0 = 0, 0.5$. It is seen that when the incident light frequency approaches the band edge the ORP for both two kinds ($\nu = 0$ and $\nu = \pm 1$) of SWCN increases rapidly. This fact may also be helpful to realize the ORP with enough intensity by tuning the proper frequency of the incident light. To have a quantitative estimation for the ORP of SWCN, we choose tubule diameter 10 \AA and the incident light wavelength 1.4 \mu m , $\phi = 0$, and $\rho = 2$, which corresponds to $\bar{\omega} \sim 0.8$ and $\Lambda \sim 13$, then the magnitude of the rotation angle per unit length can be calculated to be $79 \text{ rad/cm} \times \nu \sin(3\theta)$ for $\nu = \pm 1$ tubules and $23 \text{ rad/cm} \times \sin(6\theta)$ for $\nu = 0$ tubules.

As the final remarks, the AB effect is conventionally investigated in connection with the transport studies for the cylindrical metallic sheet. In this paper, we show that the AB oscillation will also appear in the optical phenomena generically for arbitrary chiral SWCNs. Our arguments apply even to other kinds of chiral single wall nanotubes. Moreover, the response to the enclosed magnetic flux is dramatically affected by the chiral index which characterizes different kinds of global helicity states of SWCNs and permits distinguished chirality dependence of physical properties. The gauge invariant TBA calculation not only provides quantitative results for various quantities to stimulate the experimental measurements but also verifies all the conclusions drawn from our generic symmetry analysis.

¹ Y. Aharonov and D. Bohm, Phys. Rev. **115**, 485(1959).
² M. V. Berry, Proc. R. Soc. London Ser. A **392**, 45(1984).
³ A. G. Aronov and Yu V. Shavin, Rev. Mod. Phys. **59**, 755(1987).
⁴ S. Iijima, Nature(London) **354**, 56(1991).
⁵ S. Tasaki, K. Maekawa, and T. Yamabe, Phys. Rev. B **57**, 9301(1998).
⁶ S. Reich and C. Thomsen, Phys. Rev. B **62**, 4273(2000).
⁷ R. Saito, G. Dresselhaus, and M. S. Dresselhaus, Phys. Rev. B **61**, 2981(2000).
⁸ E. L. Ivchenko and B. Spivak, Phys. Rev. B **66**, 155404(2002).
⁹ N. Sai and E. J. Mele, cond-mat/0308583
¹⁰ H. Ajiki and T. Ando, J. Phys. Soc. Jpn. **65**, 505(1996).
¹¹ J. P. Lu, Phys. Rev. Lett. **74**, 1123(1995).
¹² S. Roche, et al., Phys. Rev. B **62**, 16092(2000).

¹³ A. Bachtold, et al., Nature(London), **397**, 673(1999).
¹⁴ A. Fujiwara, et al., Phys. Rev. B **60**, 13492(1999).
¹⁵ S. Zaric, et al., Science **304**, 1129 (2004); U.C. Coskun, et al., Science **304**, 1132 (2004), these two papers are noted thanks to the referee's kindly reminder after our submission.
¹⁶ L. D. Landau and E. M. Lifshitz, *Electrodynamics of Continuous Media*, (Pergamon Press, Oxford, 1984).
¹⁷ E. J. Mele and P. Král, Phys. Rev. Lett. **88**, 056803(2002).
¹⁸ C. T. White, D. H. Robertson, and J. W. Mintmire, Phys. Rev. B **47**, 5485(1993).
¹⁹ The corresponding energy spectra of the flux threaded SWCN has been solved in the TBA in Ref. [11].
²⁰ B. A. Foreman, Phys. Rev. B **66**, 165212(2002).